

A MODEL OF STRESS ANALYSIS OF A HUMAN LONG BONE

Paulo P. Kenedi and Ivan I. T. Riagusoff

Department of Mechanical Engineering/CEFET-RJ, Rio de Janeiro, Brazil

e-mail: pkenedi@cefet-rj.br, ivanthesi@yahoo.com.br

Abstract: Bone is a very complex material, it is a living tissue that can grow, self-repair and be continuously remodeled by specialized cells that produce and remove it. Also, bone is non-homogeneous, porous and anisotropic. Nevertheless, with reasonable hypotheses it is possible to present a simple analytic stress analysis to determine, important variables as, the angles and values of principal and maximum shear stresses at external surface of a long bone submitted to a representative loading.

Keywords: stress analysis, modeling, long bones.

Introduction

A simple analytic model is proposed to describe the relationship between external loads and stresses developed at external surface of long bones, as for a human femur.

Early models [1]-[2] proposed by the authors considers a hollow circle to model a real long bone cross section. In this work an improved model that considers a hollow ellipse cross section is proposed, where long and short axis can be modified to generate better concordance with real cross sections.

A representative static loading is used as input values to the model to determine the principal stresses and the maximum shear stresses of any point of medial external bone surface. The respective angles of these stresses are also obtained

Analytic Model

This simple analytic model is constructed, based in well known stress analysis approach used in technical literature [3], to evaluate the stresses. Several restrictive hypotheses have to be made in order to assure the feasibility of the model. For instance, only cortical bone is used (the trabecular tissue is not included) to resist loading conditions, which are static. Restraints are positioned only at extremities of long bones (no side loads or side restraints are recognized) and the analysis is made at a cross section far from long bone ends.

An ellipse shape cross section, with constant thickness t , long axis $2a$ and short axis $2b$, is utilized to model a real long bone cross section, as shown at fig. 1.

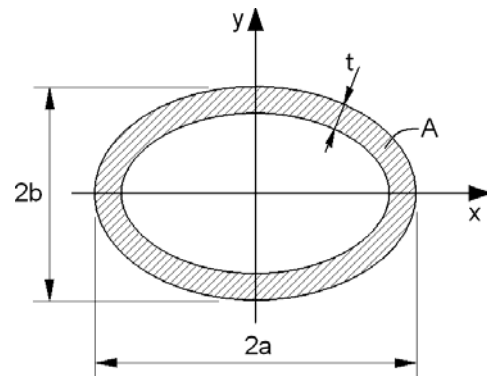


Figure 1: Idealized cross section of a human long bone.

Two coordinates systems are used for stress analysis: local and global. Local coordinates (x,y,z) are attached to cross section, where positive x axis coincide with positive long axis of cross section. Global coordinate (x^*,y^*,z^*) has always the same orientation in space, where x^*y^* is horizontal plane, x^*z^* and y^*z^* are vertical planes. Figure 2 shows the two systems of coordinates, where φ is the angle between its axes.

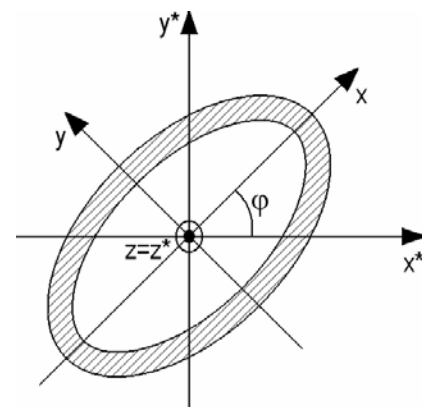


Figure 2: Two coordinates systems: local (x,y,z) and global (x^*,y^*,z^*) .

Figure 3 shows representation of a human femur hypothetical cut at a generic medial section. A concentrated load P (dashed) acts at femur head, at a distance d away from the cross section centre. Load components V_x, V_y, V_z, M_x, M_y and M_z at cross section are determined by equilibrium requirements.

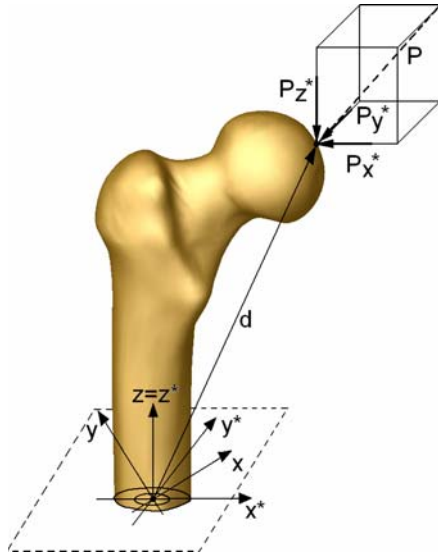


Figure 3: Loading of a human femur.

Force components, written in local coordinates, are:

$$\begin{aligned} V_x &= P_x^* \cos(\varphi) + P_y^* \sin(\varphi) \\ V_y &= -P_x^* \sin(\varphi) + P_y^* \cos(\varphi) \\ V_z &= N = P_z^* \end{aligned} \quad (1)$$

where,

$$P = P_x^* \vec{i} + P_y^* \vec{j} + P_z^* \vec{k} \quad (2)$$

Moments components, written in local system, are:

$$\begin{aligned} M_x &= M_x^* \cos(\varphi) + M_y^* \sin(\varphi) \\ M_y &= -M_x^* \sin(\varphi) + M_y^* \cos(\varphi) \\ M_z &= M_z^* = T \end{aligned} \quad (3)$$

where,

$$\begin{aligned} M_x^* &= d_y P_z^* - d_z P_y^* \\ M_y^* &= d_z P_x^* - d_x P_z^* \\ M_z^* &= d_x P_y^* - d_y P_x^* \end{aligned} \quad (4)$$

and,

$$d = d_x \vec{i} + d_y \vec{j} + d_z \vec{k} \quad (5)$$

where, N is the axial force, V is the shear force, M is the bending moment and T is the torque. The axial stress σ_N is [3]:

$$\sigma_N = \frac{N}{A} \quad (6)$$

$$A = \pi t(a + b - t) \quad (7)$$

where, A is the ellipse shape cross section area, as shown at fig. 1.

Figure 4 shows the variables used to estimate bending stresses components σ_{F_x} and σ_{F_y} , respectively, in relation x and y axis, which expressions are [3]:

$$\sigma_{F_x} = \frac{M_x y_f}{I_x} \quad (8)$$

$$\sigma_{F_y} = \frac{M_y x_f}{I_y} \quad (9)$$

where,

$$x_f = r_e \cos(\gamma) \quad (10)$$

$$y_f = r_e \sin(\gamma) \quad (11)$$

$$r_e(\gamma) = \sqrt{\frac{a^2 b^2}{a^2 \sin^2(\gamma) + b^2 \cos^2(\gamma)}} \quad (12)$$

$$I_x = \frac{\pi}{4} (ab^3 - (a-t)(b-t)^3) \quad (13)$$

$$I_y = \frac{\pi}{4} (a^3 b - (a-t)^3 (b-t)) \quad (14)$$

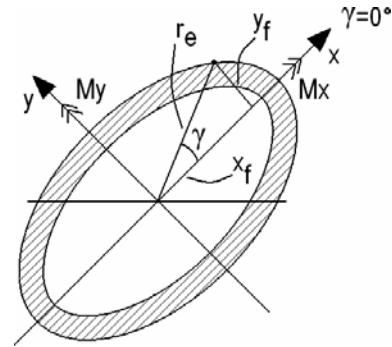


Figure 4: Bending variables.

where, x_f and y_f are, respectively, the perpendicular distances from neutral axis y and x to external bone surface, I_x and I_y are, respectively the second moment of area about x and y axis, r_e is the distance from the centre of cross section and the point of interest. γ is the angle between positive x axis and the point of interest.

Figure 5 shows the variables used to estimate torsional stress, for thin-walled cross section, which expressions are [3]:

$$\tau_t = \frac{T}{2t\hat{\Omega}} \quad (15)$$

$$\hat{\Omega} = \frac{\pi}{4} (2a-t)(2b-t) \quad (16)$$

where, $\hat{\Omega}$ is the area inside the dashed line (pass in the middle of t), shown at fig. 5.

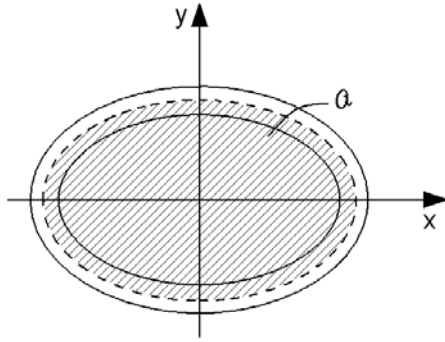


Figure 5: Torsional variables.

The figure 6 shows the variables used to estimate transverse shear stress, which expressions are [3]:

$$\tau_{v_x} = \frac{V_x Q_y}{I_y t_y} \quad (17)$$

$$\tau_{v_y} = \frac{V_y Q_x}{I_x t_x} \quad (18)$$

$$Q_x = \begin{cases} \frac{2}{3} b^2 r_e(\gamma) \cos(\gamma) \\ \frac{2}{3} \left[\left(\frac{b}{a} \right)^2 (r_e(\gamma) \cos(\gamma))^3 - \left(\frac{b-t}{a-t} \right)^2 \left((r_e(\gamma) \cos(\gamma)) - t \right)^3 \right] \end{cases} \quad (19)$$

$$Q_y = \begin{cases} \frac{2}{3} a^2 r_e(\gamma) \sin(\gamma) \\ \frac{2}{3} \left[\left(\frac{a}{b} \right)^2 (r_e(\gamma) \sin(\gamma))^3 - \left(\frac{a-t}{b-t} \right)^2 \left((r_e(\gamma) \sin(\gamma)) - t \right)^3 \right] \end{cases} \quad (20)$$

$$t_x = \begin{cases} 2 r_e(\gamma) \cos(\gamma) \\ 2 \left(r_e(\gamma) \cos(\gamma) - (a-t) \sqrt{1 - \left(\frac{r_e(\gamma) \sin(\gamma)}{b-t} \right)^2} \right) \end{cases} \quad (21)$$

$$t_y = \begin{cases} 2 r_e(\gamma) \sin(\gamma) \\ 2 \left(r_e(\gamma) \sin(\gamma) - (b-t) \sqrt{1 - \left(\frac{r_e(\gamma) \cos(\gamma)}{a-t} \right)^2} \right) \end{cases} \quad (22)$$

The limits of applicability for expressions (19) and (21), are, $-\gamma_x \leq \gamma \leq -(180^\circ - \gamma_x)$ or $\gamma_x \leq \gamma \leq (180^\circ - \gamma_x)$, for first line and otherwise for second line. Also the limits of applicability for expressions (20) and (22) are, $-\gamma_y \leq \gamma \leq \gamma_y$ or $-\gamma_y + 180^\circ \leq \gamma \leq \gamma_y + 180^\circ$, for first line and otherwise for second line.

$$\gamma_x = \arcsin \left(\left(1 + a^2 \left(\frac{1}{(b-t)^2} - \frac{1}{b^2} \right) \right)^{-1/2} \right) \quad (23)$$

$$\gamma_y = \arccos \left(\left(1 + b^2 \left(\frac{1}{(a-t)^2} - \frac{1}{a^2} \right) \right)^{-1/2} \right) \quad (24)$$

where, t_x and t_y are, respectively, the width of bone, at point of interest, perpendicular, respectively, to y and x axis, as shown at fig. 6. Q_x and Q_y are, respectively, the first moment of area about x and y axis.

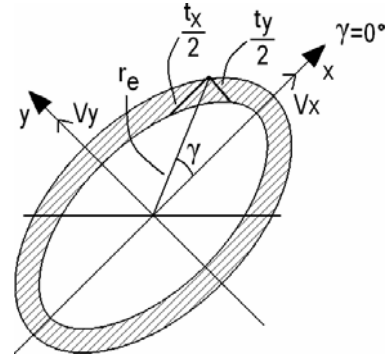


Figure 6: Transverse shear variables.

Normal and shear stresses components are combined:

$$\sigma_y = \sigma_N + \sigma_F \quad (25)$$

$$\tau_{xy} = \tau_r + \tau_v \quad (26)$$

where,

$$\sigma_F = \sigma_{F_x} + \sigma_{F_y} \quad (27)$$

$$\tau_v = \tau_{v_x} + \tau_{v_y} \quad (28)$$

Using Mohr circle approach is possible to determine the principal stresses and its respective angles. For a compressive σ_y :

$$\sigma_1, \sigma_2 = -\frac{\sigma_y}{2} \pm \sqrt{\left(\frac{\sigma_y}{2} \right)^2 + \tau_{xy}^2} \quad (29)$$

$$\theta = \frac{1}{2} \arctan \left(\left(\frac{2\tau_{xy}}{\sigma_y} \right) \right)$$

(30)

where, σ_1 and σ_2 are principal stresses, θ is the angle of σ_1 and a horizontal axis at external bone surface. Maximum shear stress $\tau_{xy_{max}}$ and its angle with the horizontal axis are:

$$\tau_{xy_{max}} = \sqrt{\left(\frac{\sigma_y}{2} \right)^2 + \tau_{xy}^2} \quad (31)$$

$$\theta' = \theta + 45^\circ \text{ or } \theta' = \theta + 135^\circ \quad (32)$$

where, θ' is the angle between $\tau_{xy_{max}}$ and the horizontal axis at external bone surface.

Results

Real loading and geometry data provided by [4] are used as input data to the proposed analytic model to predict values of principal stresses and maximum shear stresses. The loading and geometric variables are:

$$P_x^* = -420 \text{ N}, \quad P_y^* = -420 \text{ N}, \quad P_z^* = -1625 \text{ N},$$

$$d_x = 0,069 \text{ m}, \quad d_y = -0,0014 \text{ m}, \quad d_z = 0,122 \text{ m},$$

$$\varphi = 8,98^\circ, \quad a = 0,0175 \text{ m}, \quad b = 0,015 \text{ m}, \quad t = 0,0075 \text{ m}.$$

Figure 7 shows the results of application of this simple analytic model, calculated with aid of Mathcad software.

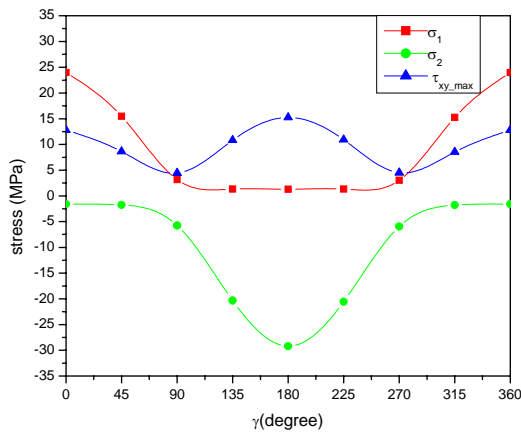


Figure 7: Distribution of principal and maximum shear stresses at a long bone external surface section.

The results of this simple analytic model were generated in steps of 45°. Note that there are two distinct behaviors, for approximately $0^\circ \leq \gamma \leq 90^\circ$ and $270^\circ \leq \gamma \leq 360^\circ$ σ_1 presents the higher positive values whereas σ_2 has small negative values. For $90^\circ < \gamma < 270^\circ$ the behavior changes, σ_1 with small positive values while σ_2 presents lower negative values. The stress magnitudes generated by the application of real data to the analytic model are coherent with elastic proprieties of bones obtained by [5] and the results of finite element of a human femur submitted by a representative loading in [6].

Discussion

The analytic approach used in this work, with restrictive hypotheses already established, results in a feasible model to describe the distribution of principal and maximum shear stresses and its respective angles, at external surface of a human long bone.

The utilization of an elliptical shape to model a cross section of a medial human femur improved the model in comparison with early models [1]-[2]. Also, the stresses obtained by this model can be used as input variables to failure criteria for long bones [7]-[9].

Finally, a finite element model, using the input provided by [4], is in development to compare the results of the analytic model. Also, it is in development the utilization of both trabecular and cortical tissues to represent a cross section of long bones.

References

- [1] Kenedi, P.P., Riagusoff, I.I.T., (2007), "A Comparative Analysis of Failures Criteria Applied to Long Bones", In: *Proceedings of 19th COBEM*, Brasilia, 5-9 Nov.
- [2] Kenedi, P.P., Riagusoff, I.I.T. (2007), "Modeling initial fracture patterns in human long bones", In: *Anais do 1º Encontro Nacional de Engenharia Biomecânica*, Petrópolis, Rio de Janeiro, 23-25
- [3] Crandall, S.H., Dahl, N. C. and Lardner, T. J., (1978), "An Introduction to the Mechanics of Solids", Second Edition with SI units, Mc Graw Hill International Editions.
- [4] Bergmann, G., Deuretzbacher, G. Heller, M., Graichen, F., Rohlmann, A., Strauss, J. and Duda, G. N., (2001), "Hip contact forces and gait patterns from routine activities", *J. Biomech.*, Vol. 34, pp.859-871.
- [5] Bayraktar, H.H., Morgan, E.F., Niebur, G. L., Morris, G. E., Wong, E.K, and Keaveny, T. M., (2004), "Comparison of the elastic and yield properties of human femoral trabecular and cortical bone tissue", *J. Biomech.*, Vol. 37, pp. 27-35.
- [6] Cilingir, A. C., Ucar, V. and Kazan, R., (2007), "Three-Dimensional Anatomic Finite Element Modeling of Hemi-Arthroplasty of Human Hip Joint", *Trends Biomater. Artif. Organs.*, Vol. 21, No. 1, pp. 63-72.
- [7] Petrtyl, M., Herf, J. and Fiala, P., (1996), "Spatial Organization of the Haversian Bone in Man", *J. Biomech.*, Vol. 29, No. 2, pp. 161-169.
- [8] Doblaré, M., García J. M. and Gómez, M. J., (2004), "Modeling bone tissue fracture and healing: a review", *Engineering Fracture Mechanics*, Vol. 71, pp. 1809-1840.
- [9] Keyak, J. H., Rosi, S.A., (2000), "Prediction of femoral fracture load using finite element models: an examination of stress – and strain-based failure theories", *J. Biomech.*, Vol. 33, pp. 209-214.